A Carbon Nanotube Cortical Neuron with Spike-Timing-Dependent Plasticity

Jonathan Joshi, Alice C. Parker, and Chih-Chieh Hsu
Ming Hsieh Department of Electrical Engineering
University of Southern California

Abstract—**This paper describes a carbon nanotube synapse circuit that exhibits Spike-Timing Dependant Plasticity (STDP). These synapses are found in cortical (e.g. pyramidal) neurons. Experiments with the synapse in a neuron circuit demonstrate changes in synaptic potential with pre- and post-spiking timing variations. The circuit design is biomimetic and changes in control voltages representing neurotransmitter concentration lead to changes in synaptic strength. The experiments are demonstrated with SPICE simulations using carbon nanotube transistor models.**

I. INTRODUCTION

Synapses, the inputs to neurons, vary their strengths with learning. A particular form of this learning is spike-timing dependent plasticity (STDP) [1], [2], [3]. With STDP, a synapse is strengthened (long-term potentiation LTP) when the presynaptic action potential at a particular synapse preceeds the postsynaptic action potential (the output of the neuron containing the synapse). A synapse is weakened (long-term depression LTD) when the postsynaptic action potential preceeds the presynaptic action potential. Thus, the temporal order of presynaptic and postsynaptic firing is a critically important aspect of STDP. The synapse is thought to be strengthened by action potentials backpropagating along the dendrites coincident with depolarization caused by a previous action potential impinging on a synapse. The backpropagation absent the previous action potential weakens the future synaptic response. In order to construct electronic neurons that learn, synapse strengthening and weakening due to STDP should be modeled.

Carbon nanotubes (CNTs) can behave as metallic wires as well as FETs. CNTs are a few nm in diameter. Current flow is largely ballistic (comparable to the flow of electrons in free space), capacitances are in attofarads, and rise and fall times in picoseconds. Channel resistance is primarily due to the quantum resistance at the junction between the nanotubes and metallic connections. Current flow between drain and source is less easily controlled than with CMOS circuits. Appropriate interfaces could be used to convert to/from biological signal levels and delays. Nanotubes induce minimum immune system reactions in living tissue [4].

This paper describes a carbon nanotube circuit implementation of a biomimetic synapse with STDP, as a part of a typical cortical neuron with a single spike (phasic). The STDP circuit detects the timing of the backpropagating action potential relative to the presynaptic action potential and induces LTP or LTD in the synapse. The STDP circuit has controls corresponding to timings of biological mechanisms. Experiments on the neuron show that when the backpropagating AP succeeds the presynaptic AP, LTP is induced otherwise LTD is induced. LTP and LTD are tested on two identical synapses of the same neuron and experiments show that the synapse undergoing LTP contributes to neural firing whereas the synapse undergoing LTD fails to contribute adequately, and the neuron does not fire. Results also show the ability to control the acceptable duration of the timing window between the backpropagating AP and the presynaptic AP.

II. BACKGROUND

There has been a keen interest in modeling synapses with STDP. Arthur and Boahen [5] model CMOS synapses that correlate and store the pre-post synchronization using an SRAM-based approach. Work done by Tovar [6] models the STDP based on Reichardt's correlation and uses the correlation towards inhibition and excitation of neighbouring neurons. Tanaka demonstrates an STDP circuit based on digital gates and flip flops to store synchronization information [7]. Work by Huo [8] shows the role of membrane threshold in their STDP synapse as a part of an integrate and fire neuron. Similar circuitry has been reported on by Indiveri et al. [9]. It differs in technology, and how biomimetic the circuits are, with less correspondence between circuit structures and biological mechanisms.

Single-walled carbon nanotubes avoid most of the scaling limits of silicon [10]. Paul *et al.* [11] demonstrated that carbon nanotube field-effect transistors (CNFETs) are less sensitive to the geometry-related process variations than silicon MOSFETs. Carbon nanotubes have the potential to be configured into 3-D arrangements, a capability we believe will become critical when implementing larger portions of the cortex due to the massive connectivity. Carbon nanotube circuits have the potential to be reconfigured in real time, a capability we feel is essential for learning. A technique has been proposed recently to design CNT circuits immune to misalignment and mispositioning that can guarantee the correct function being implemented [12]. Liu, Han and Zhou have demonstrated

1651

directional growth of high-density carbon nanotubes on a- and r-plane sapphire substrates [13]. They have developed a novel nanotube-on-insulator (NOI) approach, and a way to transfer these nanotube arrays to flexible substrates.

A CNFET device model with a circuit-compatible structure including typical device non-idealities is used in our simulations. [14]. A CMOS chip with basic neural circuits is being fabricated, and other nanotechnologies are under investigation.

III. The Carbon Nanotube Neuron Circuit

Our basic cortical neuron, shown in [15], consists of four types of sub-modules: the basic excitatory synapses ([16], [17]) the STDP synapses, the simplified dendritic arbor [17] and the axon hillock [15]. Circuit models for the dendrites and axon are not provided here. We have used two basic synapses [17] and two STDP synapses so that we can highlight the induction of LTP or LTD in each synapse, demonstrating the effect of STDP on neural firing.

A. The Excitatory Synapse, Dendritic Arbor and Axon Hillock

The work here is based on a compact, biomimetic depolarizing excitatory synapse circuit ([18], [15]), with correspondence between biological mechanisms and circuit structures. This synapse circuit evolved from an earlier synapse [17]. This circuit models cell potentials and neurotransmitter concentrations with voltages, with a correspondence between circuit elements and biological mechanisms.

Parts of the excitatory synapse circuit (Figure 1) exhibit biomimetic behavior corresponding to biological mechanisms. The action potential impinges on two sections of the synapse, namely the neurotransmitter (presynaptic) section and a mechanism (*delay 1*) that delays the neurotransmitter reuptake. The pull-up transistor in the neurotransmitter section controls the neurotransmitter concentration in the synaptic cleft (the voltage at the synaptic cleft node) while the pull-down transistor models the reuptake mechanism that controls the drop in neurotransmitter concentration in the cleft. The reuptake delay is controlled by the rise time of the delay circuit, by varying the length of its PMOS transistor to indirectly control the falling RC time constant of the neurotransmitter concentration. The neurotransmitter release causes ion channels to open; depolarization is modeled by the pull-up transistor in the receptor section tied to Vdd. The fall of the EPSP is modeled by the pull down in the same section. The time delay between the positive peak of the EPSP and its fall to ground is modeled by a second tunable delay circuit (*delay 2*). Variation in neurotransmitter concentration in the synaptic cleft causes a change in the EPSP peak amplitude, directly altering the synapse strength. The reuptake mechanism inputs *R* and *spread* control the spread of the EPSP, which modulates the temporal summation of the synapse EPSPs when successive action potentials impinge on a synapse or multiple synapses are stimulated at close intervals. The voltage across the gate labeled *Neurotransmitter_conc* controls the neurotransmitter release while the voltage across the gate *Receptor_conc* controls the receptor activation. Varying these
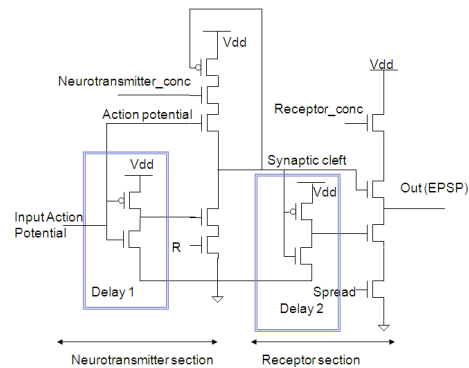

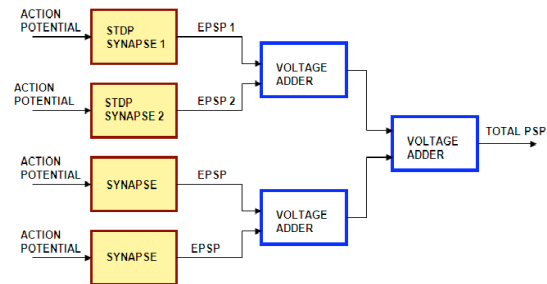Fig. 1.   The Carbon Nanotube Excitatory Synapse

Fig. 2.   The Dendritic Arbor Portion

two voltages controls the EPSP amplitude and provides an way to add circuits that exhibit plasticity.

The adder circuit in the simplified dendritic arbor [19] has been shown previously [17]. Figure 2 shows a block diagram of the dendritic arbor portion used for testing. There are four synapses (two basic and two STDP based) in the arbor, each on a separate dendritic branch. Our axon hillock circuit was described earlier [15]. Our basic neuron operates with Vdd around 0.9 V as the action potential voltage, and with 0.0 V as the resting potential. We scaled the delays with 1 ms in the biological neuron scaling to 10 ps in the nanotube neuron [20]. The postsynaptic potential at the dendritic trunk is approximately 10% of the action potential and the duration is about 6 times as long as the action potential.

B. Biomimetic STDP Circuit

The STDP circuit (Figure 3) is divided into five sections. The *NMDA Receptor Activation Section* and the *Magnesium Block Removal Section* are responsible for co-incidence detection when the presynaptic action potential (input AP) precedes the postsynaptic action potential (backpropagating AP) to induce LTP. The *NMDA Deactivation Section* and the *Calcium Channel Section* are responsible for co-incidence detection when the input AP succeeds the backpropagating AP to induce LTD. The presynaptic AP (input AP) impinges on the *NMDA Receptor Activation section* (transistor X2) to disable the LTD mechanism by raising the potential of point A and grounding the potential at B (X21) through the current mirror in the *NMDA Receptor (NMDAR) Activation Section*. The raised
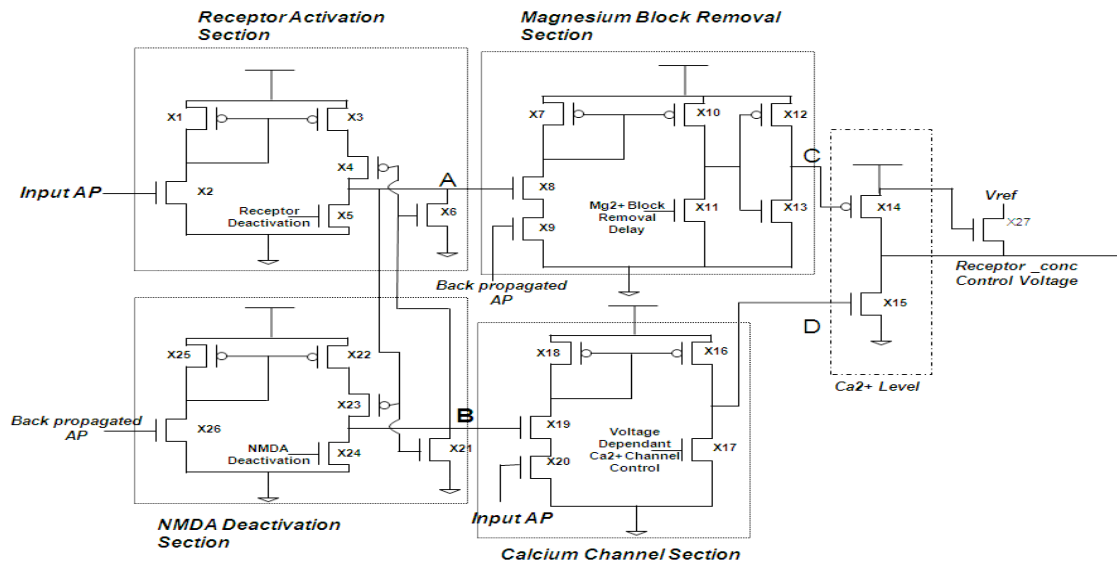
1652

Fig. 3. The STDP Circuit

potential at A also contributes to removing the magnesium block by turning on X8 in the *Magnesium Block Removal Section*. The backpropagated AP impinges on X9 completing magnesium block removal by pulling down point C through the inverting current mirror in the Block Removal section. The output of point C controls the pull up of the Ca^{2+} *Level* that controls the *receptor_conc control voltage*, (*Receptor_conc* in the synapse described in Figure 1) to induce LTP. The voltage across the gate of X5 (*Receptor Disabling*) controls the duration of time for which the synapse has the receptors activated for LTP induction (discussed in experiments). The X11 gate voltage (*Magnesium Block Removal Delay*) controls the rise time for the receptor control voltage. However when the backpropagated AP precedes the input AP it deactivates the NMDAR by turning on X26 in the *NMDA Deactivation Section* causing the rise in potential at B which pulls the A potential to ground (X6) and turns on X19. The post-pre spiking on the *calcium channel section* (X19 and X20) raises the potential at point D, pulling down the *receptor_conc control voltage* to induce LTD. The voltage across gate of X24 (*NMDA Deactivation*) controls the timing of the window for which the synapse has the receptors deactivated for LTD induction. The voltage on the gate of X17 (*Voltage Dependent Ca^{2+} Channel Control*) controls the fall time for the final receptor control voltage.

IV. EXPERIMENTS WITH THE CORTICAL NEURON

The neuron was tested with action potentials input to each synapse, and the output of the neuron measured. As shown in Figure 4, action potential 1 (dark blue trace) impinges on synapse 1 at 40 ps resulting in EPSP 1 (light blue trace). The sum of EPSP 1 and the EPSPs of synapse 3 and 4 (EPSPs kept constant at 80 mv) crosses the threshold of the neuron causing it to fire an output AP (black trace) at 70 ps as shown. This

output AP acts as the backpropagating AP for both synapses 1 and 2. Action potential 2 (dark green trace) impinges on synapse 2 at 100 ps resulting in EPSP 2 (light green trace). Synapse 1 depolarized before the backpropagating AP resulting in LTP being induced in synapse 1 as shown by the increase in the magnitude of EPSP 1 at 125 ps and 180 ps respectively. On the other hand synapse 2 undergoes LTD as shown by the decrease in the magnitude of EPSP 2 at 200 ps as a result of the presynaptic AP at 100 ps arriving too late to contribute to STDP. We tested the effects of synaptic changes on neural firing and, as shown at 180 ps, the EPSP at synapse 1 individually facilitates neural firing when added to the fixed EPSPs for synapses 3 and 4, whereas at 250 ps, the lowered EPSP at synapse 2 is too weak to cause an output spike. Figure 6 shows the effect of changing the *receptor deactivation voltage* on the STDP timing window for LTP. Changes in *NMDA Deactivation* for the LTD timing window is the same as shown in Figure 6. The changes in *Magnesium Block Removal Delay* and *Voltage Dependant Ca^{2+} Control* affect the frequency at which the backpropagating AP induces LTP or LTD. Experiments involving the relationship between spiking frequency and plasticity are the subject of a future publication. To demonstrate another aspect of plasticity we varied the voltage on the *Neurotransmitter_conc*(NT) control to change the base EPSP of the synapse. Figure 5 shows the base EPSP 1 (dotted red and blue traces) for neurotransmitter control voltages set at 0.6 v and 0.8 v respectively and EPSP 2 (solid blue and purple traces) for the same set of neurotransmitter voltages. We observe that an increase in neurotransmitter concentration leads to an increase in the base EPSP about which STDP varies.

V. CONCLUSION

A carbon nanotube cortical neuron with STDP is presented here, and simulations testing the plasticity mechanisms are
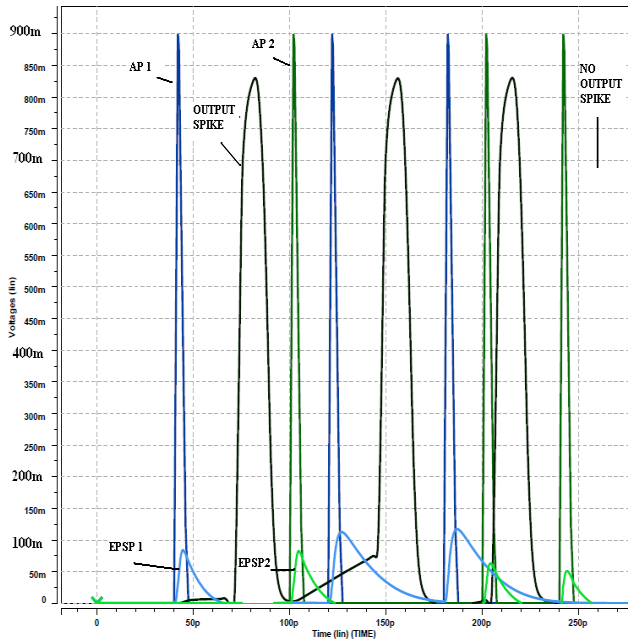
Fig. 4. Change in EPSP voltage with LTP induction in synapse 1 and LTD induction in synapse 2
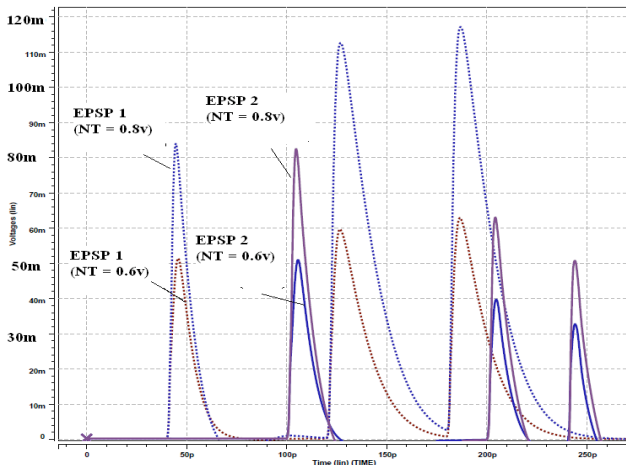

Fig. 5. Change in Base EPSP voltage with Change in Neurotransmitter Concentration
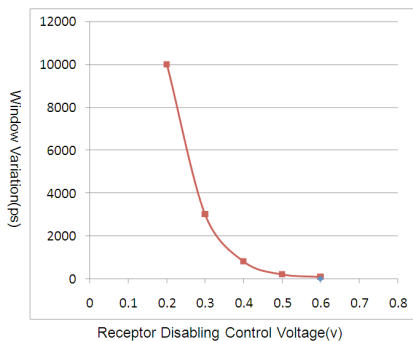

Fig. 6. Change in STDP window as receptor disabling rates change

shown. The dendritic arbor shown is vastly oversimplified. Since dendritic structural features play a major role in plasticity, these features will be taken into account in future research.

REFERENCES

[1] Y. Dan and M. M. Poo, "Spike timing-dependent plasticity of neural circuits.," *Neuron*, vol. 44, pp. 23–30, September 2004.

[2] H. Markram, J. Lübke, M. Frotscher, and B. Sakmann, "Regulation of synaptic efficacy by coincidence of postsynaptic aps and epsps.," *Science*, vol. 275, pp. 213–215, January 1997.

[3] B. M. Kampa, J. Clements, P. Jonas, and G. J. Stuart, "Kinetics of mg2+ unblock of nmda receptors: implications for spike-timing dependent synaptic plasticity.," *J Physiol*, vol. 556, pp. 337–345, April 2004.

[4] A. Bianco, R. Sainz, S. Li, H. Dumortier, L. Lacerda, K. Kostarelos, S. Giordani, and M. Prato, *Biomedical Applications of Functionalised Carbon Nanotubes*, pp. 23–50. 2008.

[5] J. Arthur and K. Boahen, "Learning in silicon: Timing is everything," in *Advances in Neural Information Processing Systems 18* (Y. Weiss, B. Schölkopf, and J. Platt, eds.), pp. 75–82, Cambridge, MA: MIT Press, 2006.

[6] G. Tovar, E. Fukuda, T. Asai, T. Hirose, and Y. Amemiya, "Analog CMOS circuits implementing neural segmentation model based on symmetric STDP learning," *Neural Information Processing*, pp. 117–126, 2008.

[7] H. Tanaka, T. Morie, and K. Aihara, "A CMOS circuit for STDP with a symmetric time window," *International Congress Series*, vol. 1301, pp. 152–155, July 2007.

[8] J. Huo and A. Murray, "The role of membrane threshold and rate in STDP silicon neuron circuit simulation," *Artificial Neural Networks Formal Models and Their Applications (ICANN 2005)*, pp. 1009–1014, 2005.

[9] G. Indiveri, E. Chicca, and R. Douglas, "A vlsi array of low-power spiking neurons and bistable synapses with spike-timing dependent plasticity," *Neural Networks, IEEE Transactions on*, vol. 17, no. 1, pp. 211–221, 2006.

[10] A. C. Parker, A. Friesz, and K. Pakdaman, "Towards a nanoscale artificial cortex," in *Proceedings of The 2006 International Conference on Computing in Nanotechnology (CNAN'06)*, June 2006.

[11] B. C. Paul, S. Fujita, M. Okajima, T. H. Lee, H. S. P. Wong, and Y. Nishi, "Impact of a process variation on nanowire and nanotube device performance," *Electron Devices, IEEE Transactions on*, vol. 54, no. 9, pp. 2369–2376, 2007.

[12] N. Patil, J. Deng, A. Lin, H. S. P. Wong, and S. Mitra, "Design methods for misaligned and mispositioned carbon-nanotube immune circuits," *Computer-Aided Design of Integrated Circuits and Systems, IEEE Transactions on*, vol. 27, no. 10, pp. 1725–1736, 2008.

[13] X. Liu, S. Han, and C. Zhou, "Novel nanotube-on-insulator (noi) approach toward single-walled carbon nanotube devices," *Nano Letters*, vol. 6, pp. 34–39, January 2006.

[14] J. Deng and H. S. P. Wong, "A circuit-compatible spice model for enhancement mode carbon nanotube field effect transistors," in *Simulation of Semiconductor Processes and Devices, 2006 International Conference on*, pp. 166–169, 2006.

[15] J. Joshi, C. Hsu, A. Parker, and P. Deshmukh, "A carbon nanotube cortical neuron withexcitatory and inhibitory dendritic computations," in *IEEE/NIH 2009 LIfe Science Systems and Applications Workshop (LiSSA 2009)*, 2009.

[16] A. K. Friesz and A. C. Parker, "A biomimetic carbon nanotube synapse," in *Biomedical Engineering Conference*, 2007.

[17] A. C. Parker, J. Joshi, C.-C. Hsu, and N. A. D. Singh, "A carbon nanotube implementation of temporal and spatial dendritic computations," in *Circuits and Systems, 2008. MWSCAS 2008. 51st Midwest Symposium on*, pp. 818–821, 2008.

[18] G. M. Shepherd, ed., *Synaptic Organization of the Brain,*, vol. 5, ch. Introduction to Synaptic Circuits. Oxford University Press, 2004.

[19] H. Chaoui, "CMOS analogue adder," *Electronics Letters*, vol. 31, no. 3, pp. 180–181, 1995.

[20] C. Yu-Ming, L. Rosene, J. Killiany, A. Mangiamele, and I. Luebke, "Increased action potential firing rates of layer 2/3 pyramidal cells in the prefrontal cortex are significantly related to cognitive performance in aged monkeys," *Cerebral Cortex*, vol. 15, pp. 409–418, April 2005.